[PS]Predicting Clearwater Formation Natural Fracture Intensity, Athabasca Oil Sands Area*

Queena Chou[1], Andres Altosaar[2], and Kevin Gillen[3]

Search and Discovery Article #51286 (2016)**
Posted August 29, 2016

*Adapted from poster presentation given at AAPG Annual Convention and Exhibition, Calgary, Alberta, Canada, June 19-22, 2016

[1]Weatherford Reservoir Solutions, Calgary, Alberta, Canada (queena.chou@ca.weatherford.com)
[2]Suncor Energy Inc., Calgary, Alberta, Canada
[3]Consultant, Burnaby, British Columbia, Canada

Abstract

This research investigates the controls on natural fracture intensity observed in Clearwater Formation over townships 94-95, ranges 5-6, west of the fourth meridian. These potential controls include thickness variations of both Clearwater Formation and underlying Devonian age rocks, as well as the topography of the sub-Cretaceous unconformity. Fracture data were drawn from 30 boreholes, all of which have both core and image log essentially covering the full thickness of Clearwater Formation. Results show that Clearwater Formation thins to the north and does not appear to influence natural fracture intensity. Where Firebag Member of Waterways Formation thins and disappears to expose Slave Point Formation subcrop in northeast corner, no correlation is observed between fracture intensity values and Devonian age formation thickness. The relationship between natural fracture intensity and the underlying sub-Cretaceous unconformity is unclear. A map view of natural fracture intensity overlaid on the sub-Cretaceous unconformity surface indicates that some of the highest intensity values occur along the transition edge from topographically high to low areas. However, fracture intensity along the transition edge is variable. Some lower intensity values occur along this same edge. If the basin edge does influence fracture development, its relationship is statistical in nature and does not manifest as a one-to-one mapping.

References Cited

Berkowitz, B., 1995, Analysis of Fracture Network Connectivity Using Percolation Theory: Mathematical Geology, v. 27/4, p. 467-483.

Davy, P., C. Darcel, O. Bour, R. Munier, and J.R. De Dreuzy, 2006, A note on the angular correction applied to fracture intensity profiles along drill core: Jour. Phys. Research: Solid Earth, American Geophysical Union, 2006, v. B11, p. 111.

Englman, R., Y. Gur, and Z. Jaeger, 1983, Fluid flow through a crack network in rocks: Jour. Appl. Mech., v. 50, p. 707-711.

McLellan, P.J., K.P. Gillen, and S. Rogers, 2014, Essential Elements of Caprock Integrity Assessment for Thermal Recovery Projects: AAPG-CSPG Oil Sands & Heavy Oil Symposium: A Local to Global Multidisciplinary Collaboration, Calgary, Alberta, October 14-16, 2014.

Ozkaya, S.I., and J. Mattner, 2003, Fracture connectivity from fracture intersections in borehole image logs: Computers & Geosciences, v. 29, p. 143-153.

Robinson, P.C., 1983, Connectivity of fracture systems--a percolation theory approach: Jour. Phys. A: Math. Gen., v. 16/3, p. 605-614.

Schneider, C.L., S. Mei, K. Haug, and M. Grobe, 2014, The sub-Cretaceous unconformity and the Devonian subcrop in the Athabasca Oil Sands area, townships 87–99, ranges 1–13, west of the fourth meridian: AER/AGS Open File Report 2014-07.

Terzaghi, R.D., 1965, Sources of error in joint surveys: Geotechnique, v.15, p. 287-304.

Tsui, P.C., M. Cruden, and T.S. Thomson, 1989, Ice-thrust terrains and glaciotectonic settings in central Alberta. Can.J. of Earth Sci., v. 26, p. 1308-1318.

Wang, X., 2005, Stereological Interpretation of Rock Fracture Traces on Borehole Walls and Other Cylindrical Surfaces: PhD dissertation, Virginia Polytechnic Institute and State University, Blacksburg, Virginia.

Predicting Clearwater Formation Natural Fracture Intensity, Athabasca Oil Sands Area

Authors: **Queena Chou**, Weatherford Reservoir Solutions
Andres Altosaar, Suncor Energy Inc.
Kevin Gillen, Consultant

Abstract

This research investigates the controls on natural fracture intensity observed in the Clearwater Formation over townships 94-95, ranges 5-6, west of the Fourth Meridian. These potential controls include thickness variations of both the Clearwater Formation and underlying Devonian age rocks, as well as the topography of the sub-Cretaceous unconformity. Fracture data were drawn from 30 boreholes, all of which have both core and image logs, essentially covering the full thickness of the Clearwater Formation. Results show that the northward erosional thinning of the Clearwater Formation does not appear to influence natural fracture intensity. No correlation is observed between fracture intensity values and the Devonian Waterways and Slave Point subcrop transition. The relationship between natural fracture intensity and the underlying sub-Cretaceous unconformity is unclear. A map view of natural fracture intensity overlaid on the sub-Cretaceous unconformity surface indicates that relatively high intensity values occur along the transition edge from topographically high to low areas. However, fracture intensity along the transition edge is variable. Some lower intensity values occur along this same edge. If the basin edge does influence fracture development, its relationship is statistical in nature and does not manifest as a one-to-one mapping.

Geological Setting

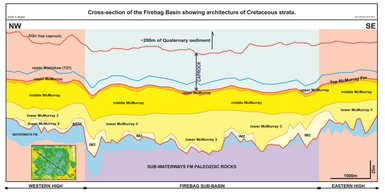

Figure 1: Cross-section of Firebag Basin

Located 60 km northeast of the city of Fort McMurray, Alberta, Canada, the Firebag Basin is host to bitumen saturated siliciclastics of the Aptian McMurray Formation. These deposits form a portion of Suncor Energy's resource at the Firebag Steam-Assisted Gravity Drainage (SAGD) Project. A northwest–southeast cross-section shows the Firebag Basin's architecture of Cretaceous age rock strata in relation to the sub-Cretaceous unconformity (Figure 1). Devonian carbonates of the Waterways Formation, the Slave Point Formation and older Paleozoic strata make up the rock mass beneath the unconformity. The Clearwater Formation serves as the regional caprock for the SAGD operation. Above the Clearwater Formation lies a thin interval consisting of Grand Rapids Formation mudstones. A 200-meter (m) thick blanket of undifferentiated glacial and post-glacial Quaternary sediments lies unconformably above the Cretaceous succession.

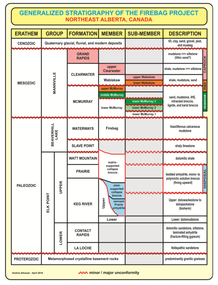

Figure 2: Firebag Stratigraphy

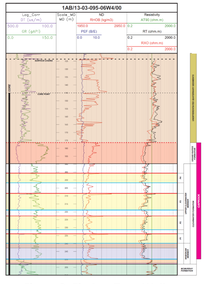

Figure 3: Firebag Type Well

Figure 2 shows the generalized stratigraphy of Firebag SAGD Project. Regional pervasive sub-Cretaceous unconformity separates Cretaceous Period McMurray Formation reservoir, Clearwater and Grand Rapids Formation caprocks. Below sub-Cretaceous unconformity Devonian Period Waterways Formation Firebag Member is observed in Firebag Basin. Beneath Firebag Member an unconformity is observed at top of Slave Point Formation in Firebag Basin. Matrix-supported collapse breccia resulted from salt dissolution in Prairie Evaporite Formation lies beneath Slave Point Formation. At the base, Prairie Evaporite consists of clast-supported solution breccia and remnant of anhydrite. Figure 3 shows the detailed stratigraphy of the caprock succession for the Firebag SAGD Project. The caprock interval consists of three units: the informal upper Wabiskaw member, the informal upper Clearwater member, and the Grand Rapids Formation. Upper Wabiskaw member and upper Clearwater member caprock strata are clay-rich, laterally extensive marine deposits. The Grand Rapids Formation consists of clayey shales. This presentation focusses on natural fracture intensity data from only the Clearwater Formation.

Figure 4 shows regional variation and extensiveness of salt dissolution (modified from Schneider et al. 2014). The Firebag Basin lies in the purported zone of total dissolution, however remnant anhydrites of the Prairie Evaporite Formation are still present within, and in thicknesses of up to 25m. Figure 5 shows a map of the sub-regional tectonic setting (structure on the sub-Cretaceous unconformity modified from Schneider et al., 2014). Although rooted in Precambrian basement rocks, the Firebag Basin is most prominently expressed at the sub-Cretaceous unconformity (SCU). Negative relief on this surface is upwards of 50m, and defines a nearly equidimensional rhombic basin with sharp margins. The overall surface area of the basin is upwards of 45 km^2, and its shape is reflected in all underlying geologic surfaces. Regional potential field data sets highlight a major 100 km long, NNW-SSE linear discontinuity transecting the Firebag SAGD Project that is interpreted to be a fault at the level of the Precambrian basement. Higher resolution aeromagnetic data coupled with 3D seismic suggest the fault is strike-slip in nature, locally segmented and contains both paired bend and potential bypass structures. The structural history of the Firebag Basin is subdivided into four distinct phases: 1- Paleoproterozoic (Taltson-Thelon orogeny), 2- Early-Middle Devonian (extension associated with uplift of the Peace River-Athabasca Arch and Antler orogeny), 3- Middle Jurassic to Early Cretaceous (Sevier-Columbia orogenies), 4- Early Cretaceous (Columbia-early Laramide orogenies). Paleozoic compressional events are interpreted to have preferentially activated this regional strike-slip fault in a dextral sense, promoting both extensional and contractional regimes within the study area. The Firebag Basin formed in the extensional zone developed around the northern releasing bend. The corresponding contractional zone formed around the southern restraining bend is defined by basement uplift and erosion. Mesozoic basement fault activation is interpreted to have significantly accelerated and focused the episodic dissolution of Middle Devonian evaporite. The Firebag Basin is described here as a composite pull-apart/karst basin that owes its origin to sub-regionally unique extensional responses to regional compressional tectonics, and non-unique multi-phase evaporite dissolution-collapse.

Core and Image Log

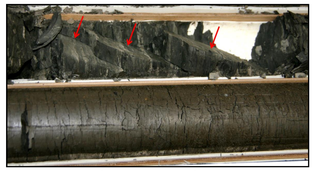

Figure 6: (a) 1AA/01-16-095-06W4/00. Natural fractures Observed in Upper Clearwater Member. Unmineralized Fractures at 247mKB TVD. Arrows Indicate Fractures

In terms of fractures, faults and bedding, we use the same definitions of Bates and Jackson (1984). Assessment of fracture origin in core (i.e. natural versus coring-induced) was primarily accomplished using fracture shape and surface textures (fractography).

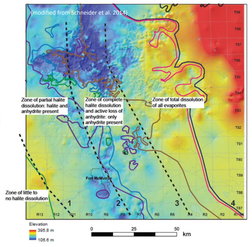

Figure 4: Regional Salt Dissolution Map

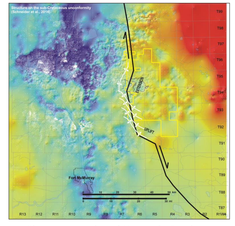

Figure 5: Regional Tectonic Setting

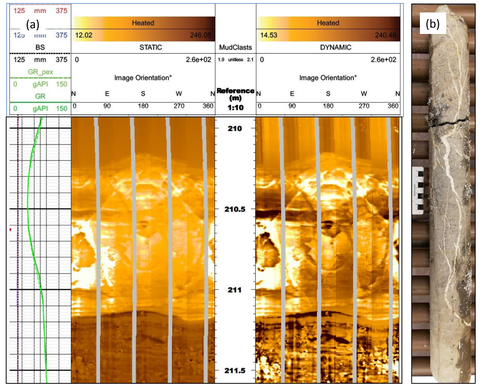

Figure 7: (a) 100/02-07-095-06W4/00. Resistive Fractures Interpreted from Siltstone 210.4–211.2 mKB TVD, Upper Clearwater member (b) Associated Siltstone in Core Showing Multiple Mineralized Fractures

Methods

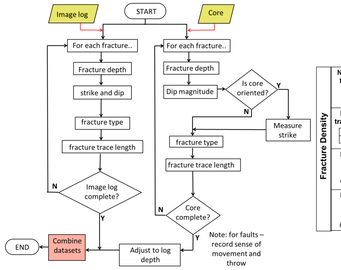

Figure 8: Flowchart for creation of master data set for a borehole (modified from McLellan et al. 2014)

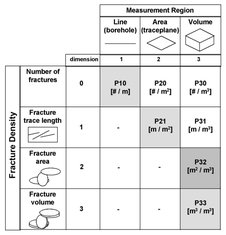

Figure 9: Fracture Intensity Measures (source: Golder Associates Ltd. 1995)

Table 1: Methods for Correction of Directional Sampling Bias

Method	Required Values	Estimate	Attributes	Reference
1	Dip magnitude, and Observed P_{10}	corrected P_{10}	Correction goes infinite as β begins to parallel borehole axis	Terzaghi (1965)
2	Fracture height, core (borehole) diameter, core (borehole) length	corrected P_{10}	Individual fracture sets must be identified before application	Narr (1996)
3	Dip magnitude, and Observed P_{10}	corrected P_{10}	Requires accurate definition of mechanical unit thickness	Narr and Lerche (1984)
4a	Mean Fisherian pole, precision parameter (k), Observed P_{10}	P_{32}	Correction goes infinite as β begins to parallel borehole axis when k is high	Wang (2005)
4b	Mean Fisherian pole, k, Observed $P_{31,C}$	P_{33}	Correction varies between 1 and π/2	Wang (2005)

Each of the 30 boreholes examined in this study have both core and resistivity-based image logs. Some boreholes have additional acoustic-based image logs. After analysis for fractures and faults, data from these sources were combined. Depth shifting of core was performed for each core tube, followed by matching of discontinuity data between sets. This "bookkeeping" phase ensures that any individual feature is not counted more than once, and produces a "master dataset" (Figure 8). In the same borehole, image log (which reflects the borehole wall) and core have different diameters and sampling volumes. Although not sensu stricto with respect to some statistical sampling methods, we feel that the benefits realized from combining fracture datasets acquired from two sources greatly outweighs any potential drawbacks. In our opinion, the combined fracture dataset more accurately reflects the nature of rock mass compared to either core or image log data on their own. Figure 9 shows several measures of fracture intensity. The standard measure of fracture frequency in a borehole (the observed number of fractures/m or P10) is subject to directional sampling bias. Table 1 lists some of the methods available for correcting for directional sampling bias. Method 1 Terzaghi correction for bias tends to overcorrect in cases where fractures are subparallel to the borehole/core axis (Davy et al., 2006). Only P32 (fracture area per unit volume, m^2/m^3) and P33 (fracture volume per unit volume, m^3/m^3) are immune from directional sampling bias. All fracture intensity data have been converted to P32 values to compensate for directional sampling bias. The details of the method are outlined in Wang, 2005.

Fracture Intensity

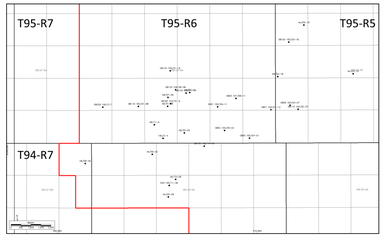

Figure 10: Well Locations of Analyzed Caprock Data

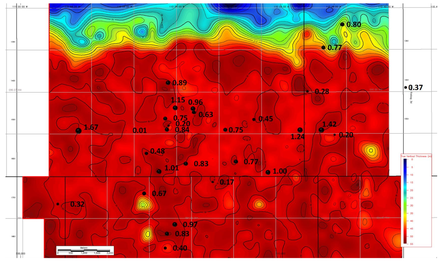

Figure 11: Natural fracture intensity P32 values in caprock overlaid on Clearwater Formation isopach map

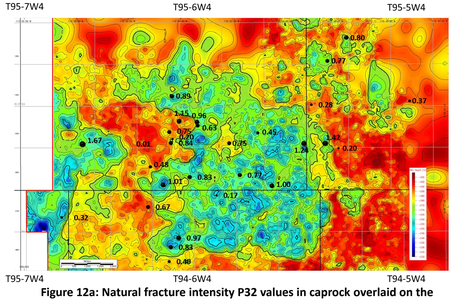

Figure 12a: Natural fracture intensity P32 values in caprock overlaid on the sub-Cretaceous unconformity structure map

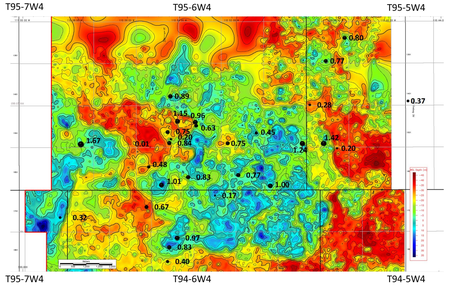

Figure 12b: Natural fracture intensity P32 values in caprock overlaid on the sub-Cretaceous unconformity first residual structure map

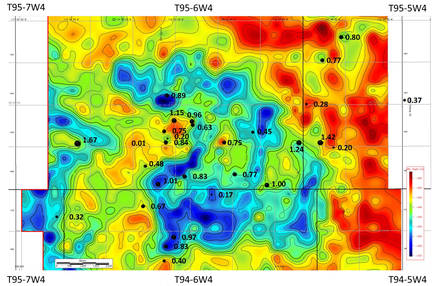

Figure 13a: Natural fracture intensity P32 values in caprock overlaid on McMurray Formation reservoir structural map

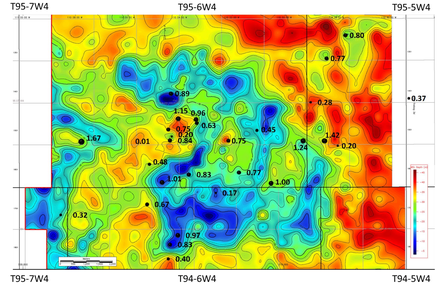

Figure 13b: Natural fracture intensity P32 values in caprock overlaid on McMurray Formation reservoir first residual structural map

Figure 10 shows the well locations of investigated boreholes in this study. When considering the variability of natural fracture intensity in the Clearwater Formation, thickness variability of the formation is examined. Figure 11 shows an isopach map of the Clearwater Formation. The thickness of the Clearwater Formation ranges between 35 and 55 meters, and abruptly thins to the north due to glacial erosion. P32 data is overlaid at investigated borehole locations and are represented in bubble map format. Diameters of bubbles are proportional to the P32 intensity value for each borehole. The influence of underlying structures are investigated by plotting P32 data on top of contoured maps of underlying surfaces. P32 data overlay structural maps and associated first residual structure maps of the sub-Cretaceous unconformity, and the McMurray Formation. A residual structure map highlights the difference between the structural top and the regional slope, which brings out local effects. Structural contours are shown in five meter intervals.

The highest P32 estimate is 1.67 m^2/m^3 at 100/02-07-095-06W4/00. This borehole is positioned close to eastern edge of Firebag Basin pictured in Figures 12 and 13. Similar in character to variation in P32 values around the edge of central low, the eastern edge of basin also shows a lower P32 value of 0.32 m^2/m^3 at 1AB/08-36-094-07W4/00. Figures 12 and 13 suggest both higher and lower P32 values can be found close to the edge of central low. It is possible underlying structure influences fracture intensity, but the relationship may be obscured by the statistical nature of fracture development. Based on P32 data overlay on structural maps and Clearwater Formation isopach map, natural fracture intensity is variable between boreholes and cannot be correlated to underlying structure or caprock thickness. Values to the north of basin are generally comparable to values to the south of basin, despite the northward thinning of caprock.

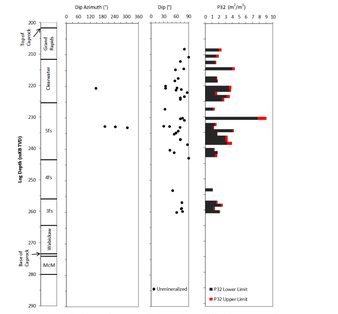

Figure 14: Variation of Estimated P32 Values with Depth in 100/02-04-095-06W4/00

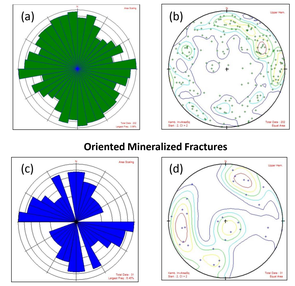

Figure 15: Oriented Fracture Field Data

Figure 14 shows a typical profile of P32 estimates within a borehole. 100/02-04-095-06W4/00 estimated P32 of 1.06 m^2/m^3 in the Clearwater Formation. Figure 15 shows rose plots of natural fracture strikes observed in investigated boreholes from Firebag. The number of fractures presented is significantly smaller than the total dataset of observed natural fractures, since only fully oriented fractures, i.e., fractures documented from borehole image logs can be plotted, and three slant cores in which all recorded data are fully oriented. Upper hemisphere pole-to-plane plots suggest the possibility of weak development of groupings within individual boreholes. However, orientations of fracture populations can be quite variable between boreholes, so much so that oriented fracture datasets approach random state in their distributions. This potentially complicates prediction of fracture orientation.

Summary

- The relationship between intensity and underlying structure is unclear. Since such a relationship would be expected to be statistical, a one-to-one mapping may not be apparent even in cases where underlying structure has an influence on P32.
- Within boreholes, intensity is variably developed with depth.
- Mineralized fractures observed within Clearwater Formation core may not contribute to hydraulic flow.
- Rose plots of fracture strike suggest the possibility of weak development of groupings within individual boreholes.
- Variation between boreholes exists and complicates prediction of fracture orientation.
- There does not appear to be a strong relationship between fracture/fault orientation and the underlying sub-Cretaceous unconformity. If a relationship does exist, it may be obscured by the statistical spread in the data.

References

Berkowitz, B. (1995): Analysis of Fracture Network Connectivity Using Percolation Theory, Mathematical Geology, 27. No. 4, 467-483.

Dney, P., Darcel, C., Bour, O., Munier, R., De Dreuzy., J.R., (2006) A note on the angular correction applied to fracture intensity profiles along drill core. Jour. Phys. Research: Solid Earth, American Geophysical Union, 2006, 811, 111 pp.

Englman, R., Gur, Y., and Jaeger, Z. (1983): Fluid Flow through a crack network in rocks. Jour. Appl. Mech., v. 50, p. 707-711.

McLellan, P.J., Gillen, K.P., and Rogers, S. (2014): Essential Elements of Caprock Integrity Assessment for Thermal Recovery Projects. AAPG-CSPG Oil Sands & Heavy Oil Symposium: A Local to Global Multidisciplinary Collaboration, Calgary, Alberta, October 14-16.

Oshaya, S. L., and Mattner, J. (2003): Fracture connectivity from fracture intersections in borehole image logs. Computers & Geosciences, 29, 143-153.

Robinson, P. C. (1983): Connectivity of fracture systems--a percolation theory approach. Jour. Phys. A: Math. Gen., v. 16, no. 3, p. 605-614.

Schneider, C.L., Mei, S., Haug, K., and Grobe, M. (2014) The sub-Cretaceous unconformity and the Devonian subcrop in the Athabasca Oil Sands area, townships 87–99, ranges 1–13, west of the fourth meridian. AER/AGS Open File Report 2014-07

Terzaghi, R. D. (1965): Sources of error in joint surveys. Geotechnique, v.15, 287-304.

Tsui, P.C., Cruden, M., and Thomson, T.S. (1989): Ice-thrust terrains and glaciotectonic settings in central Alberta. Can.J. of Earth Sci., 26, 1308-1318.

Wang, X. (2005, September): Stereological Interpretation of Rock Fracture Traces on Borehole Walls and Other Cylindrical Surfaces. PhD dissertation, Virginia Polytechnic Institute and State University, Blacksburg, Virginia.

Acknowledgement: Authors thank Suncor Energy Inc. for approval of data release.